

Candesartan ameliorates brain inflammation associated with Alzheimer's disease

Nofar Torika¹ | Keren Asraf¹ | Ron N. Apte² | Sigal Fleisher-Berkovich¹ 

¹Department of Clinical Biochemistry and Pharmacology, Ben-Gurion University of the Negev, Beersheba, Israel

²Department of Microbiology and Immunology, Ben-Gurion University of the Negev, Beersheba, Israel

Correspondence

Sigal Fleisher-Berkovich, Department of Clinical Biochemistry and Pharmacology, Ben-Gurion University of the Negev, Beersheba, Israel.

Email: fleisher@bgu.ac.il

Funding information

This work was supported by the Israel Science Foundation (grant no. 101/11-16).

Summary

Aims: Alzheimer's disease (AD) pathology is associated with brain inflammation involving microglia and astrocytes. The renin-angiotensin system contributes to brain inflammation associated with AD pathology. This study aimed to investigate the role of candesartan, an angiotensin II type 1 receptor blocker, in modulation of glial functions associated with AD.

Methods: Focusing on the role of candesartan in glial inflammation, we evaluated inflammatory mediators' levels, secreted by lipopolysaccharide-induced microglia following candesartan treatment. Also, short-term intranasal candesartan effects on amyloid burden and microglial activation were investigated in 5 familial AD mice.

Results: Candesartan showed anti-inflammatory effects and shifted microglial activation toward a more neuroprotective phenotype. Candesartan decreased the lipopolysaccharide-induced nitric oxide synthase and cyclooxygenase-2 expression levels, which was accompanied by an induction of arginase-1 expression levels and enhanced A β_{1-42} uptake by microglia. Moreover, intranasally administered candesartan to AD mice model significantly reduced the amyloid burden and microglia activation in the hippocampus.

Conclusions: These results thus shed light on the neuroprotective role of candesartan in the early stage of AD, which might relate to modulation of microglial activation states.

KEYWORDS

Alzheimer's disease, angiotensin II, candesartan, glial inflammation

1 | INTRODUCTION

Brain inflammation is a neuropathological hallmark of Alzheimer's disease (AD).¹ Inflammatory processes in AD involve amyloid β (A β) depositions, as well as the activation of glia and, to a less extent, of neurons.^{2,3} In AD brains, microglia are located nearby A β plaques.⁴ This interaction is deleterious to neurons as A β promotes microglia to secrete pro-inflammatory cytokines and reactive oxygen species to the surrounding brain tissues.³ As microglia display a range of activation profiles, they could conceivably also play a neuroprotective role in the disease.⁴ Indeed, microglia were reported to phagocytose A β , to

release anti-inflammatory mediators and neurotrophic factors, and to participate in tissue repair.^{5,6}

Recently, the 5 familial Alzheimer's disease (5XFAD) mouse model was used in several brain inflammation and AD studies.^{7,8} AD-like features rapidly appear in the brain of 5XFAD mice, including A β deposits, gliosis, brain inflammation, impaired memory and neuronal loss. The amyloid plaques, and proportionally, gliosis, initially appear in specific brain areas when the mice reach the age of 2 months. No changes were observed in cognitive functions of 2- to 4-month-old 5XFAD mice.⁹

The classical renin-angiotensin system (RAS) was initially described as a peripheral hormone system that plays a major role in

regulation of body fluid homeostasis and cardiovascular system.¹⁰ However, accumulating evidence for the existence of an independent brain RAS prompted the search for additional physiological roles for this system.¹¹

The major biologically active peptide generated by RAS is angiotensin II (Ang II).¹² Ang II functions as a pleiotropic neuroregulator that stimulates 2 receptor types, the AT1 (AT1R) and AT2 (AT2R) receptors, both distributed in the brain.^{13–16} Increased brain AT1R stimulation can be pathological, leading to brain inflammation and neuronal injury.¹⁷ Not surprisingly, common pro-inflammatory signaling cascades were found to be involved in the activation of AT1R and of Toll-like receptor 4 (TLR4) by Ang II and the endotoxin, lipopolysaccharide (LPS), respectively.¹³

Modulation of brain inflammation associated with AD by angiotensin-related drugs has been the subject of great interest over recent years.^{13,16} Indeed, Ang II AT1R blockers (ARBs) are potent anti-inflammatory compounds that exert neuroprotective effects.^{16,18,19} Increasing evidence suggests that ARBs may be effective therapeutic agents for brain diseases, including AD and Parkinson's disease (PD).^{16,20} Recent studies conducted on AD transgenic mice models indicated preventive effects for AT1 receptor blockage on AD hallmarks.^{21–23} Most of these rodent studies demonstrated neuroprotective and anti-inflammatory features for ARB treatment. Nevertheless, ARBs effect on A β load seems to change depending on administration procedure, AD model, and the dose used. Danielyan et al²¹ showed reduced brain A β levels in APP/PS1 transgenic mouse model following intranasal losartan treatment. However, Ongali et al²² reported no alteration in amyloid levels in APP mice treated with losartan in drinking water. Previously, ARBs were reported as modulators of macrophages polarization in different tissues.^{24–26} However, the role of brain RAS in microglial polarization toward neuroprotective phenotype is less clear.²⁷ We and others showed induction of neuroprotection through microglial polarization by telmisartan.^{18,28} In PD mouse model, ARB treatment protected from dopaminergic neurons death, reduced motor deficits, and inhibited microglial activation.^{29,30} Candesartan (a blood-brain barrier-entering ARB) reversed the neurotoxic effects of AT1R overstimulation in animal models of systemic inflammation.^{31–34} Candesartan, subcutaneous administered, to LPS-injected hypertensive or normotensive rats decreased the LPS-induced gliosis in the brain parenchyma.^{32–34} Interestingly, a recent study indicated a great neuroprotective potential for candesartan in AD as it affected the expression of hundreds of genes in AD patients' cortex and hippocampus.³¹

The effect of candesartan on A β expression in AD mouse brains has been hardly investigated before. In this study, we investigated the effect of intranasal treatment with candesartan on disease pathology in the 5XFAD mouse brain. Candesartan was introduced to 2-month-old 5XFAD mice, when amyloid deposition and gliosis begin. Moreover, the effect of candesartan, studied here, on modulation of microglial polarization is not known.²⁷ Finally, we investigated for the first time, whether candesartan influences A β uptake by microglial cells.

2 | MATERIALS AND METHODS

2.1 | Cell culture

2.1.1 | BV2 microglial cells

BV2 microglial cells, a kind gift from Prof. Rosario Donato (Department of Experimental Medicine and Biochemical Sciences, University of Perugia, Italy), were grown as detailed.¹⁹

2.1.2 | Neonatal rat primary microglia and mixed glial cells cultures

Isolated primary microglia and mixed glial cells comprising astrocytes and microglia were obtained from whole brain of 0- to 24-hour-old rat pups. Cell cultures were grown as detailed.¹⁹ To obtain primary mixed glial cultures, 1×10^6 cells per well were cultured in poly-L-lysine-coated, 24-well plates for 21 days. The medium was removed, and fresh medium was replaced twice weekly. For microglia isolation, 35×10^6 mixed glial cells were cultured in flasks, and medium was replaced once a week. On day 12, flasks were shaken, and floating microglia were recultured in 24-well plates, 10^6 cells per well.

Prior to experiment, medium was replaced with fresh serum-free medium (SFM; pH 7.4), and the cells were incubated for further 4 hour. Test agents in SFM were added containing 0.1% bovine serum albumin (BSA) and 10 mmol/L HEPES buffer for the indicated times.

LPS and actinomycin D were purchased from Sigma-Aldrich (St. Louis, MO) (Cat No. L2880 and A9415), and candesartan cilexetil was purchased from Tocris Bioscience (Bristol, UK) (Cat No. 4972).

2.2 | Mice

The 5XFAD model mice were used. This model harbors 3 familial AD (FAD) mutations in the human APP695 and 2 mutations in the human presenilin-1 genes.⁹ Animals were housed in cages as detailed.¹⁸ Mice, 2 months of age, were placed in a supine position and treated intranasally every day, for 8 weeks, with candesartan or vehicle (3 μ L drop to each nostril). Candesartan was dissolved in *N,N*-dimethylformamide/polyethylene glycol 400/saline (2:6:2) solvent at a concentration of 2 mg/mL.³⁵ Mice were randomly divided into 3 treated groups as following: (i) 1 mg/kg/d candesartan Tocris Bioscience (Bristol, UK) (Cat No. 4971)-treated wild-type (WT) mice ($n = 6$), (ii) 1 mg/kg/d candesartan-treated 5XFAD mice ($n = 8$), and (iii) vehicle-treated 5XFAD mice ($n = 7$). Candesartan-treated WT mice were chosen as the control group, representing the pattern of both candesartan-treated and vehicle-treated WT groups.

All animal procedures were approved by the Institutional Animal Care and Use Committee of the Ben-Gurion University of the Negev (approval numbers IL-30-08-2011-15 and IL-54-08-2015-19).

2.3 | Cell viability

Cell viability was determined by a Cell Proliferation Kit (XTT) (Biological Industries, Kibbutz Beit-Haemek, Israel) (Cat No. 20-300-1000) according to the manufacturer's instructions. The assay was performed using a microplate reader (Bio-Rad model 680).

2.4 | Assessing A β uptake by flow cytometry

Cells were pre-incubated with 1 μ mol/L or 5 μ mol/L candesartan cilexetil or SFM for 20 hour at 37°C. Thereafter, 0.5 μ mol/L (for BV2 cells) or 0.75 μ mol/L (for primary microglia) of Hilyte Fluor 488-labeled A β ₁₋₄₂ (AnaSpec, Cat No. 60479-01) was added for another 2 hours. The supernatant was removed; cells were rinsed with cold phosphate buffer solution (PBS), detached, and collected. Primary microglial cells were stained for microglial markers using PE-vio-770-conjugated rat anti-CD11b/c and APC-conjugated rat anti-CD45 antibodies (Miltenyi Biotec, Germany) (Cat No. 130-105-318 and 130-107-843). CD11b/c⁺/CD45⁺ and intracellular fluorescence of A β ₁₋₄₂ were analyzed by flow cytometry (GuavaTech, Chicago, IL). Different doses of A β ₁₋₄₂ were used in the experiments, chosen according to calibration curve. Cytochalasin D (Sigma-Aldrich, Cat No. 22144-77-0) was used as A β uptake inhibitor.

2.5 | Nitric oxide (NO) production levels

The Griess reaction was used to measure supernatant nitrite concentration as an indicator of NO production. Well supernatant was mixed with an equal volume of Griess reagent (Sigma-Aldrich, Cat No. G4410) in a 96-well plate and incubated for 15 minutes. Mixture absorbance was measured at 540 nm using a microplate reader (model 680, Bio-Rad, Hercules, CA). NO levels were normalized to cell numbers.

2.6 | Enzyme-linked immunosorbent assay (ELISA)

Supernatant tumor necrosis factor- α (TNF- α), transforming growth factor- β 1 (TGF- β 1) (Cat No. DY410 and DY1679), and interleukin 1- β (IL1- β) (Cat No. 559603) levels were assayed using ELISA kits (R&D Systems, Minneapolis, MN and BD Biosciences, San Diego, CA) according to the manufacturers' instructions.

2.7 | SDS-PAGE gel electrophoresis and Western blot analysis

Whole-cell and whole-brain protein extracts were obtained using lysis buffer following rinsing or cold PBS cardiac perfusion, respectively. Lysates were subjected to 7.5% or 10% PAGE and transferred onto nitrocellulose membranes. Membranes were blocked with 4% BSA and incubated overnight at 4°C with the following antibodies: rabbit anti-inducible nitric oxide synthase (iNOS) (1:500, Cayman Chemicals, Ann Arbor, MI, Cat No. 160862), rabbit anti-arginase-1 (Arg-1) (1:200, Santa Cruz Biotechnology, Dallas, TX, Cat No. SC-166920), rabbit anti-mouse cyclooxygenase-2 (COX-2) (1:1000,

Abcam, Cambridge, UK, Cat No. ab15191), rabbit anti-CD10/neprilysin (NEP) (1:4000, Abcam, Cambridge, UK, Cat No. ab73409), rabbit anti-insulin-degrading enzyme (IDE) (1:4000, Calbiochem, Merck Millipore, Billerica, MA, Cat No. AB9210) and for protein load normalization, mouse anti- β -actin (1:4000, Sigma-Aldrich, Cat No. A2228). The corresponding conjugated antibodies were added for 90 minutes: donkey anti-rabbit (1:10 000, GE Healthcare, Buckinghamshire, UK, Cat No. NA9340) or horseradish peroxidase-conjugated goat anti-mouse (1:20 000, Jackson ImmunoResearch, West Grove, PA, Cat No. 115-005-003). Immunoreactivity was revealed as detailed.¹⁸

2.8 | Immunohistochemistry

Mice were anesthetized, and cardiac perfusion was performed. One brain hemisphere was removed and incubated in 4% paraformaldehyde (PFA) solution following by a 30% sucrose solution. Forty- μ m-thick cryostat sagittal brain sections were obtained from -80°C frozen tissues in tissue adhesive (O.C.T compound, Tissue-Tek, Torrance, CA). Sections were rinsed and blocked using antibody diluting buffer (GBI labs, Bothell, WA). Immunohistochemical staining for A β peptides and CD11b markers was performed using rabbit anti-human A β antibodies (1:250, kind gift from Professor Alon Monsonogo, Ben-Gurion University) and rat anti-mouse/human CD11b antibodies (1:25, Biolegend, San Diego, CA, Cat No. 101201). The appropriate secondary antibodies were used: Cy3-conjugated donkey anti-rabbit IgG (1:1000, Jackson ImmunoResearch Laboratories, Cat No. 711-165-152) or Alexa fluor 488-conjugated goat anti-rat IgG (1:250, Jackson ImmunoResearch, Cat No. 112-545-003). Mounting medium containing DAPI (Vector labs, Burlingame, CA) was used for counterstaining. Images were obtained using the Olympus FluoView FV1000 confocal microscope (Olympus, Hamburg, Germany) at a 1024 \times 1024-pixel resolution with \times 10 objective.

2.9 | Imaging analysis

A β plaque and CD11b staining in hippocampal and cortical areas were quantified in 5 brain sections from each individual mouse using ImageJ software (version 1.40C, NIH) with the threshold function. Five determinations of cortex and five of hippocampus per mouse were taken for quantification. Fluorescence intensity (basal levels) was first obtained in sections from control mice (WT). An intensity threshold was set to mark only those areas showing significant staining. Identical laser-scanning parameters were used for all samples. The averaged positive-stained areas for the indicated proteins were calculated separately for each treated group.

2.10 | Statistical analysis

Data are presented as the mean \pm SEM. Significance assessment (considered at $P < 0.05$) between experimental groups was determined using one-way analysis of variance (ANOVA) followed by post hoc multiple comparison test (Tukey-Kramer multiple comparison test).

3 | RESULTS

3.1 | Candesartan with or without LPS does not show any cytotoxic effect in BV2 microglial cells

We first examined the effect of candesartan on viability of BV2 microglial cells (Figure 1). We used actinomycin D, a cell proliferation inhibitor, as positive control. Actinomycin D (0.5 $\mu\text{g}/\text{mL}$) significantly inhibited BV2 proliferation by 98%. Candesartan (1 $\mu\text{mol}/\text{L}$ and 5 $\mu\text{mol}/\text{L}$), LPS (7 ng/mL), or both compounds given together do not show any cytotoxic effect in BV2 microglia (Figure 1).

3.2 | Candesartan decreases LPS-induced NO, TNF- α , and TGF- β 1 but not IL1- β release from microglial cells

The extent to which candesartan can serve as an anti-inflammatory compound in microglia was investigated by taking measurements of inflammatory cytokine production levels following LPS stimulation. We stimulated BV2 microglia (Figure 2A,C-E) or primary mixed glial cells (Figure 2B) with LPS and measured nitrite (Figure 2A,B), TNF- α , TGF- β 1, and IL1- β (Figure 2C-E) levels. LPS increased production of nitrite in BV2 microglia (Figure 2A) and in primary mixed glial cells (Figure 2B). The addition of 1 $\mu\text{mol}/\text{L}$ or 5 $\mu\text{mol}/\text{L}$ candesartan reduced LPS-induced NO levels in BV2 cells by 19% and 83%, respectively (Figure 2A). Greater attenuation of NO levels by candesartan was observed in primary mixed glial cells. Here, addition of 1 $\mu\text{mol}/\text{L}$ or 5 $\mu\text{mol}/\text{L}$ of the compound reduced NO levels by nearly 53% and

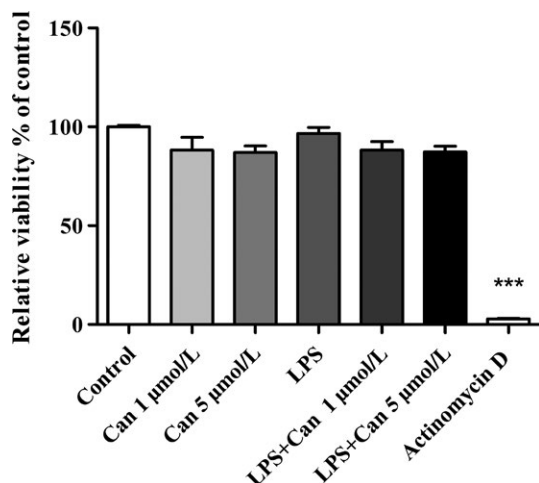


FIGURE 1 Effect of candesartan with or without LPS on viability of BV2 microglial cells. Cells were incubated with either actinomycin D (0.5 $\mu\text{g}/\text{mL}$) or candesartan (Can) (1 $\mu\text{mol}/\text{L}$ or 5 $\mu\text{mol}/\text{L}$) alone or in combination with 7 ng/mL LPS for 24 h. At the end of the experiment, viability was assessed by the XTT assay. Results are given as mean \pm SEM of 2 independent experiments ($n = 2$ experiments, each experiment included 12 samples for treatment). One-way ANOVA and a Tukey-Kramer multiple comparison test were used to test for statistical significance. *** $P < 0.001$ vs control (nonstimulated cells)

87%, respectively (Figure 2B). Treatment with 1 $\mu\text{mol}/\text{L}$ candesartan did not significantly alter TNF- α or TGF- β 1 levels in BV2 microglia (Figure 2C,D). However, application of 5 $\mu\text{mol}/\text{L}$ candesartan attenuated LPS-induced TNF- α and TGF- β 1 levels by up to 68% and 48%, respectively (Figure 2C,D). Although LPS induced the production of IL1- β from BV2 microglia in more than 2-fold, candesartan treatment did not affect its levels (Figure 2E). Candesartan alone did not alter basal production of NO, TNF- α , TGF- β 1, and IL1- β in glial cultures (Figure 2A-D insets).

3.3 | Candesartan decreases the expression of pro-inflammatory markers and promotes the expression of an anti-inflammatory marker in LPS-stimulated BV2 cells

We next investigated whether blockage of the AT1R in BV2 cells by candesartan would affect the expression levels of pro- and anti-inflammatory enzymes. iNOS, COX-2, and Arg-1 levels were measured in LPS-induced BV2 cells following 24-hour treatment with candesartan. iNOS (Figure 3A) and COX-2 (Figure 3B) expression levels were significantly elevated in LPS-stimulated BV2 cells by 100% and 39%, respectively, when compared to control. Candesartan treatment resulted in a dose-dependent manner attenuation of the expression levels of these proteins. Exposure to 1 $\mu\text{mol}/\text{L}$ or 5 $\mu\text{mol}/\text{L}$ candesartan reduced LPS-induced iNOS expression levels by 48% and 82% (Figure 3A), while COX-2 expression levels were significantly attenuated upon addition of 5 $\mu\text{mol}/\text{L}$ candesartan by approximately 45% (Figure 3B). On the other hand, LPS treatment reduced the expression levels of Arg-1 by 90%, as compared to control (Figure 3C). Treatment with 5 $\mu\text{mol}/\text{L}$ candesartan abrogated the LPS-mediated effect on Arg-1 expression levels, with expression levels reaching 60% higher of LPS (Figure 3C). Candesartan treatment did not alter iNOS, Arg-1, and COX-2 expression levels as compared to nontreated control cells (data not shown).

3.4 | Intranasal administration of candesartan reverses A β pathology and microglial activation in the hippocampus layer of 5XFAD mice

As candesartan modulated LPS-induced inflammation in glial cells, we investigated whether microglial modulation and anti-inflammatory effects associated with AD are also be demonstrated in the brain of 5XFAD mice. Accordingly, 1 $\text{mg}/\text{kg}/\text{d}$ candesartan or the vehicle was administered intranasally into 2-month-old 5XFAD mice for 8 weeks. The load of microglial accumulation and amyloid burden expression were assessed immunohistochemically in brain cortical and hippocampal sections. Cortical (Figure 4A,B,E,F) and hippocampal (Figure 4C,D,G,H) areas of 5XFAD mice treated intranasally with the vehicle were observed to express high levels of A β (Figure 4A-D) and CD11b (Figure 4E-H) staining. As expected, no A β staining (Figure 4A-D) and only minor staining for the CD11b marker (Figure 4E-H) was observed in the brain sections of WT mice. Candesartan significantly reduced amyloid burden expression levels in the hippocampal layer

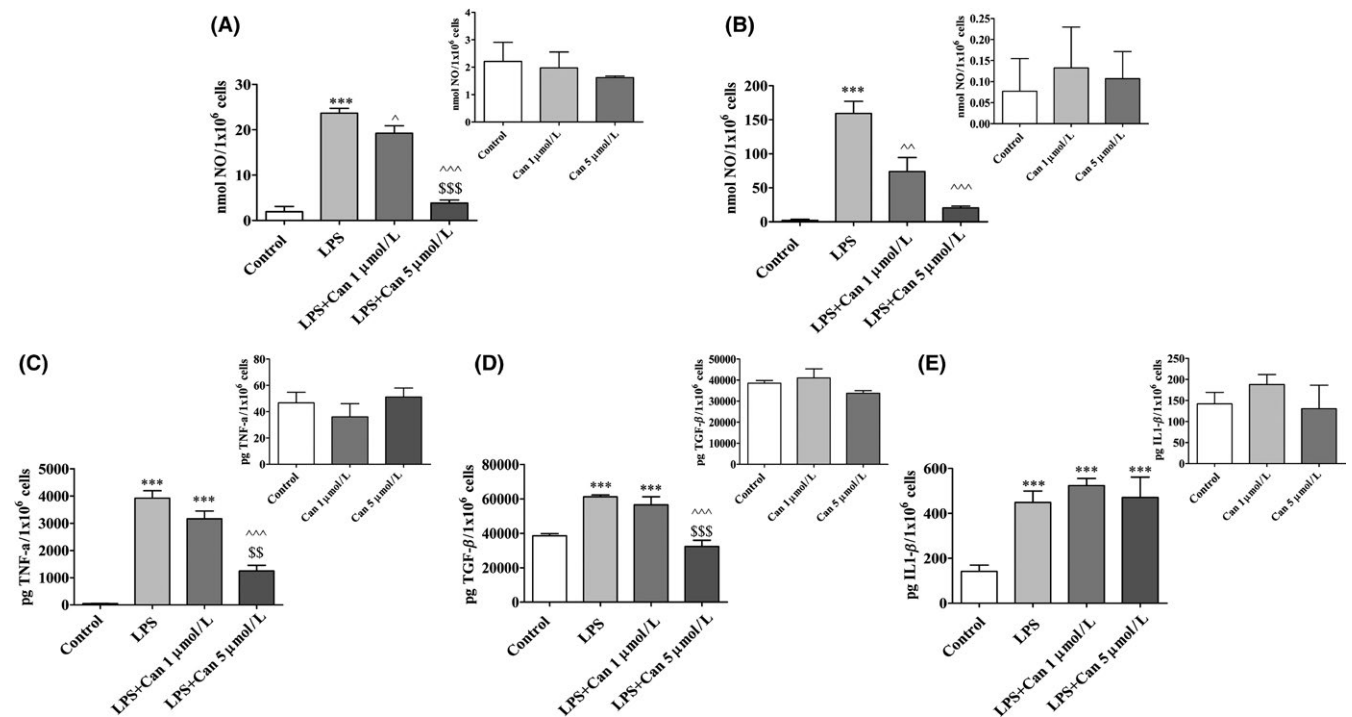


FIGURE 2 Candesartan decreased NO, TNF- α , and TGF- β 1 but not IL1- β production by microglial cells. BV2 microglial cells (A,C-E) and mixed glial cells (B) were incubated for 24 h with 7 ng/mL or 0.5 μ g/mL LPS, respectively, in the presence or absence of 1 or 5 μ mol/L candesartan (Can). Supernatants were analyzed for NO (A, B) TNF- α (C), TGF- β 1 (D), and IL1- β (E) levels and normalized to cell counts. *Insets:* NO (A-B), TNF- α (C), TGF- β 1 (D), and IL1- β (E) levels measured in nonstimulated cells treated with Can at 1 μ mol/L or 5 μ mol/L concentrations. Means \pm SEM of representatives of 3 (A-B) or 2 (C-E) independent experiments are presented (A-B: $n = 3$ experiments, each experiment included 24 samples for treatment; C-E: $n = 2$ experiments, each experiment included 18 samples for treatment). One-way ANOVA and a Tukey-Kramer multiple comparison test were used to test for statistical significance. *** $P < 0.001$ vs control (nonstimulated cells); $^{\wedge}P < 0.05$ vs LPS; $^{\wedge\wedge}P < 0.01$ vs LPS; $^{\wedge\wedge\wedge}P < 0.001$ vs LPS; $^{\$}P < 0.01$ vs LPS+1 μ mol/L candesartan; $^{\$ \$ \$}P < 0.001$ vs LPS+1 μ mol/L candesartan

of 5XFAD mice by 45% compared to age-matched vehicle-treated 5XFAD mice (Figure 4C,D). However, this effect was not observed in the cortical layer of candesartan-treated 5XFAD mice (Figure 4A,B). Similarly, 30% reduction in the area stained for CD11b in the hippocampal sections of 5XFAD mice was observed following candesartan treatment (Figure 4G,H). Candesartan administration did not alter the calculated area stained for CD11b in the cortical layer compared to the area measured in the vehicle-treated group (Figure 4E,F).

3.5 | Candesartan does not affect A β -degrading enzyme expression levels in 5XFAD-treated mice brains

Next, we investigated whether A β clearance by candesartan is associated with induced expression levels of A β -degrading enzyme. Whole-brain protein lysates from 5XFAD or WT mice treated with candesartan or the vehicle were measured for NEP and IDE protein levels. The expression levels of NEP were dramatically reduced in the brains of 5XFAD-treated mice by more than 2-fold, when compared to brains of age-matched WT mice (Figure 5A). However, no significant alterations in NEP expression levels were observed between the 2 5XFAD-treated groups following candesartan or vehicle treatment (Figure 5A). Similarly, intranasal administration of candesartan did not affect IDE expression levels in the brains

of 5XFAD-treated mice, as compared to vehicle-treated mice (Figure 5B).

3.6 | Candesartan induces A β phagocytosis by microglia

As candesartan did not affect the amyloid burden load via changes in degrading enzyme levels, we considered an alternative mechanism for A β clearance by assessing A β phagocytosis analysis in microglial cells (Figure 6). The uptake of labeled A β ₁₋₄₂ peptides by BV2 cells was examined following A β peptide treatment in the presence or absence of candesartan and cytochalasin D by FACS. Labeled A β ₁₋₄₂ uptake by BV2 reached saturation in the presence of 1 μ mol/L peptide (Figure 6A). Two-hour treatment with 0.5 μ mol/L (for BV2 cells) or 0.75 μ mol/L (for primary microglia) A β ₁₋₄₂-labeled peptide induced about 21% of BV2 and 10% of primary microglial cells to phagocytose the peptide, relative to the signal observed with nontreated cells (Figure 6B,E, respectively). Pretreatment with candesartan resulted in significant increase in phagocytosis of A β ₁₋₄₂ by BV2 (Figure 6B,C) and primary microglial (Figure 6E,F) cells. 10 μ mol/L cytochalasin D inhibited A β uptake in BV2 cells by 80%-90% when administered with or without candesartan (Figure 6B,C). Candesartan treatment did not significantly alter the inhibitory effect of cytochalasin D on A β uptake as phagocytosis inhibition levels were similar in the presence or absence of candesartan.

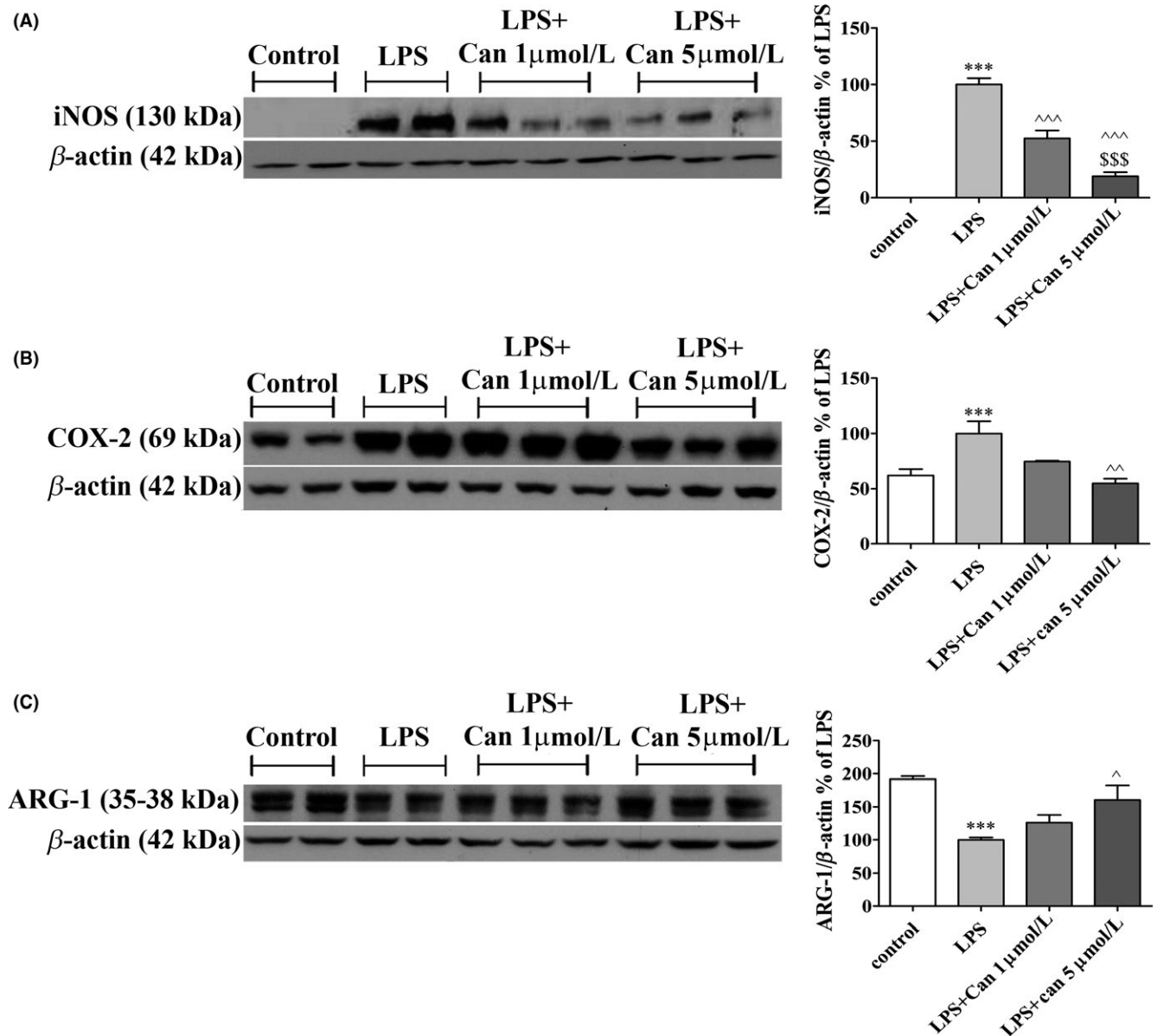


FIGURE 3 Candesartan decreased the inflammatory response and elevated anti-inflammatory factors' expression in LPS-induced microglia. BV₂ Cells were incubated for 24 h with LPS (7 ng/mL) in the presence or absence of 1 or 5 μ mol/L candesartan (Can). Whole-cell protein lysates were prepared and relative levels of iNOS (130 kDa) (A), COX-2 (69 kDa) (B), and ARG-1 (35–38 kDa) (C) were determined by Western analysis using target-specific primary antibodies and compared to β -actin (42 kDa) levels. Means \pm SEM of representatives of 3 independent experiments are presented (n = 3 experiments, each experiment included 2–3 samples for treatment). One-way ANOVA and a Tukey–Kramer multiple comparison test were used for statistical significance. *** P < 0.001 vs control (nonstimulated cells); ^^ P < 0.001 vs LPS; ^^ P < 0.01 vs LPS; ^ P < 0.05 vs LPS; \$\$\$ P < 0.001 vs LPS+1 μ mol/L candesartan

4 | DISCUSSION

Microglial cells are the major cellular regulators of innate immune responses in the central nervous system (CNS).^{2,36} Brain injury and neurodegenerative diseases shift microglia toward an activated phenotype.³⁶ LPS induces brain inflammation which is associated with glial cells activation.³⁷ LPS and A β peptides may both activate microglia through the same receptors, namely TLR4 and CD14.^{38,39} During the host defense response, activated glial cells release neurotoxic factors, such as TNF- α , IL1- β , and NO.^{40,41}

In the present study, candesartan was shown to reduce the production of NO, TNF- α , and TGF- β 1 but not of IL1- β (Figure 2) in LPS-induced glial cells. Benikey et al³³ showed reduced IL1- β levels in 4-hour LPS-stimulated cortical microglia (100 ng/mL) following 2-hour pretreatment with candesartan (10 μ mol/L). In the present study, a 24-hour treatment with candesartan did not change IL1- β release compared to LPS (7 ng/mL)-stimulated BV2 microglial cells. Changes in modulation of IL1- β release between studies may be due to different concentrations and incubation times with LPS and candesartan. A similar effect of candesartan on TNF- α and nitrite levels in inflammation-induced

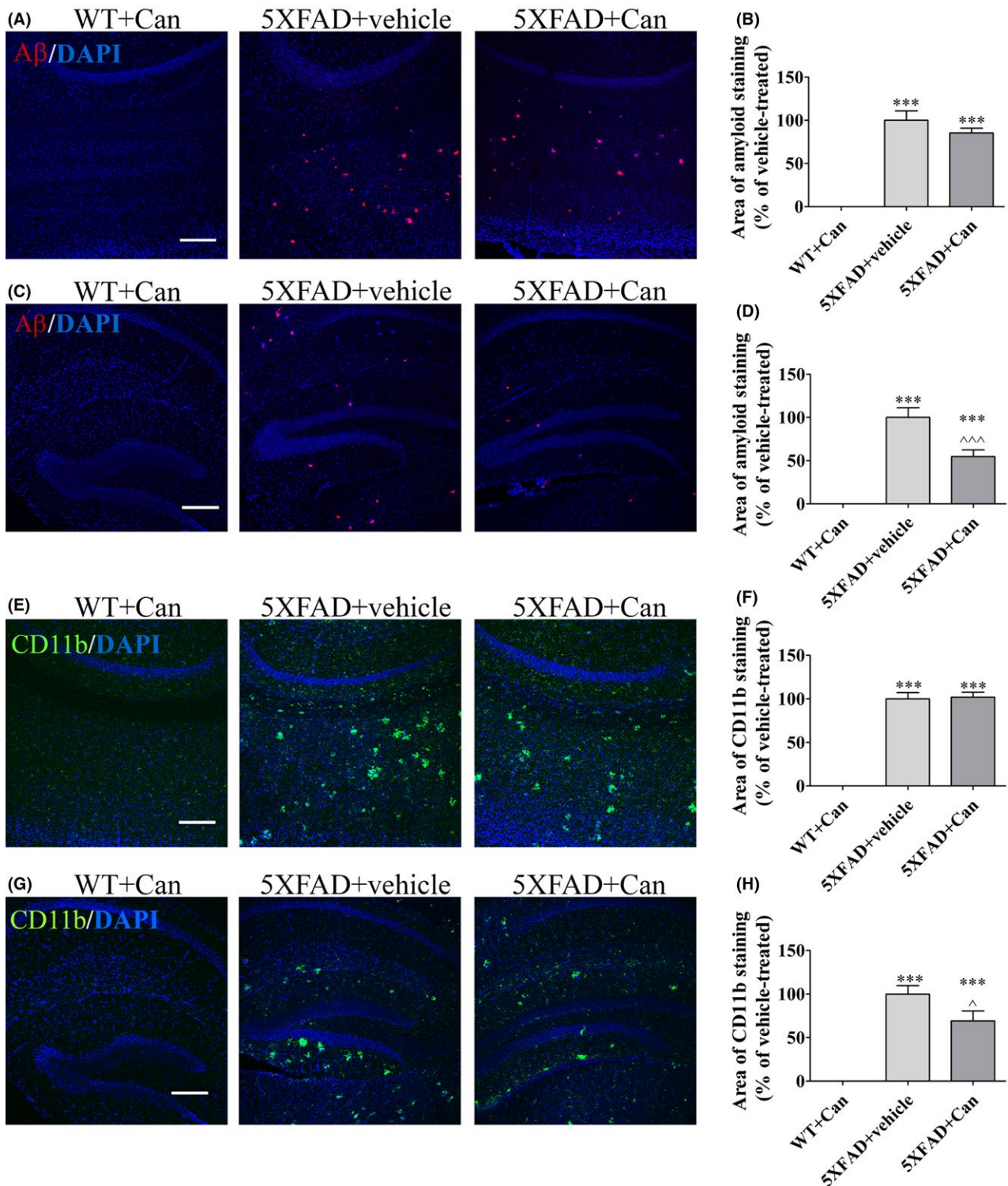


FIGURE 4 Candesartan reduced A β expression and microglial activation in the hippocampus of 5XFAD mice. Eight-week-old mice were treated intranasally with either candesartan (Can) or the vehicle for 2 mo. At the end of the experiment, the mice were sacrificed, cardiac perfusion was performed, and brain sections were obtained. Sections were immunolabeled with anti-CD11b (green) and anti-A β (red) antibodies and counterstained with DAPI (blue). Representative cortical (A, E) and hippocampal (C, G) layers from WT or 5XFAD mice treated with candesartan (1 mg/kg/d) or with the vehicle are shown. The experiment included 6–8 mice per group ($n = 21$ in total). The average sums of A β -stained (B, F) and of CD11b-stained (D, H) areas were quantified and are represented as the mean \pm SEM percentage of the stained area in the corresponding vehicle-treated group in at least 3 repeats. Statistical significance was determined using one-way ANOVA, followed by a Tukey–Kramer multiple comparison test. *** $P < 0.001$ vs WT+Tel; ^^ $P < 0.001$ vs 5XFAD+vehicle; ^ $P < 0.05$ vs 5XFAD+vehicle. Scale bar is 200 μ m

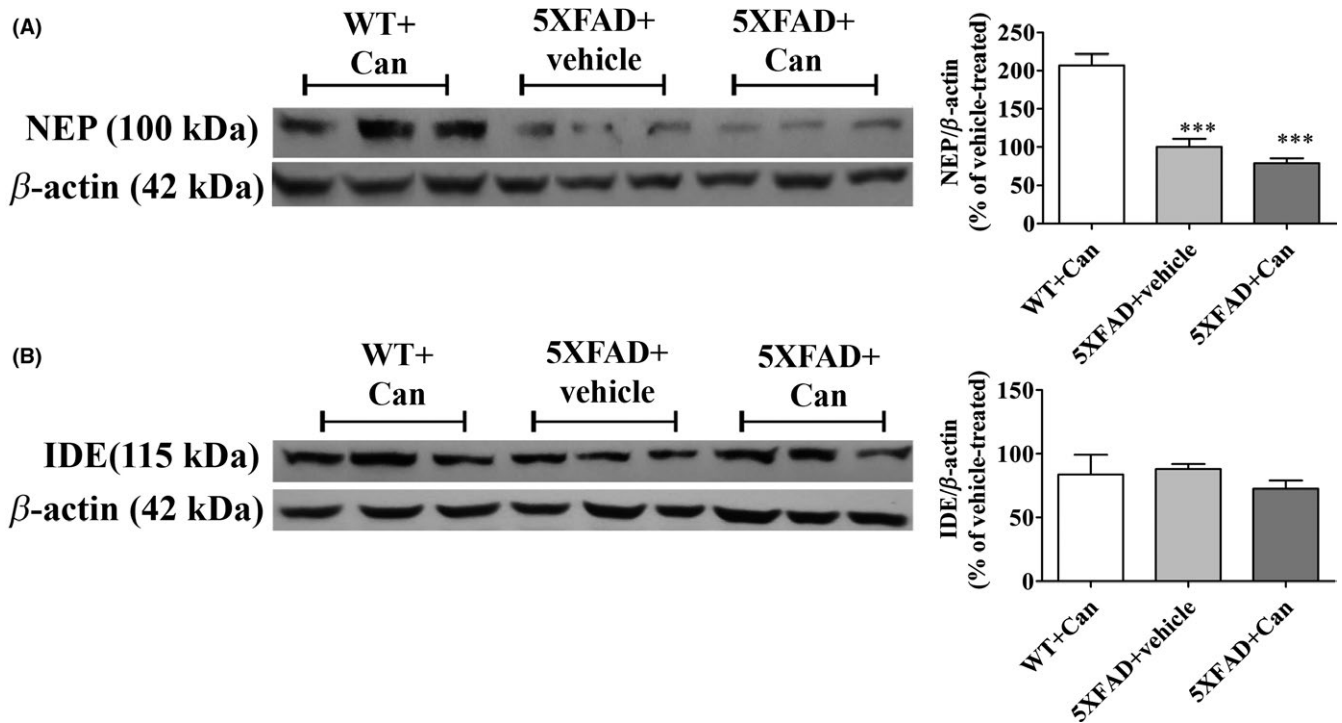


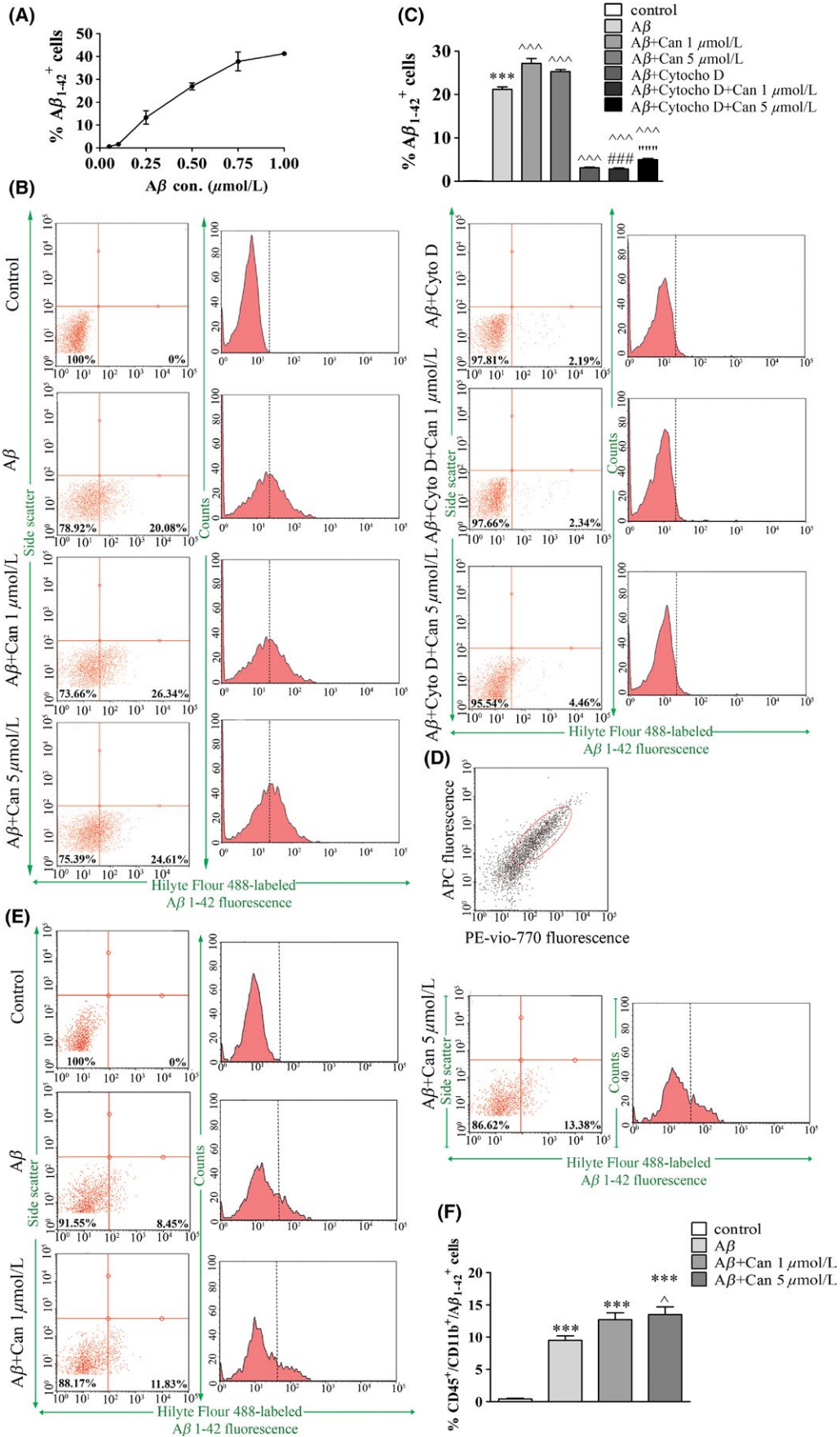
FIGURE 5 Intranasal administration of candesartan does not alter NEP or IDE expression levels in the brains of 5XFAD mice. Eight-week-old mice were treated intranasally with either candesartan (Can) or the vehicle for 2 mo. At the end of the experiment, the mice were sacrificed and whole-brain protein lysates were prepared and levels of NEP (100 kDa) (A), IDE (115 kDa) (B) proteins were determined relative to β -actin (42 kDa) levels by Western analysis using target-specific primary antibodies. Representative blots and graphs from wild-type (WT+Can) or 5XFAD mice treated with 1 mg/kg/d candesartan (Can) (5XFAD+Can) or with the vehicle (5XFAD+Vehicle) are shown. Means \pm SEM of representatives of 6–8 mice per group ($n = 21$ in total) are presented. One-way ANOVA and a Tukey-Kramer multiple comparison test were used for statistical significance. *** $P < 0.001$ vs WT+Can

isolated glial cell lines was shown by Bhat et al.⁴² TGF- β 1 is an inflammatory cytokine that plays a dual role in T cells during inflammation, with its role being determined by the surrounding cell milieu.⁴³ Lanz et al.⁴⁴ suggested that during neuroinflammation, microglia are the main producers of TGF- β 1 in the CNS and are highly responsive to Ang II. The reduction in TGF- β 1 levels following candesartan treatment shown in our study is in agreement with Lanz et al, whose study focused on the role of AT1R in chronic progressive experimental autoimmune encephalomyelitis (EAE) and showed a decrease in TGF- β 1 production following candesartan treatment in primary glial cells.⁴⁴

As part of their functional plasticity, microglia can induce the production of anti-inflammatory cytokines, together with phagocytosis of cellular debris.⁴⁵ ARG-1 is one of several cell integrity-associated

markers that are expressed as microglia assume a neuroprotective phenotype.⁴⁶ As ARG-1 and iNOS compete for the same substrate, arginine, enhanced expression of ARG-1 may result in reduced microglial release of NO.⁴⁷ Phagocytosis of A β by microglia also serves a neuroprotective role in the brain.⁴⁵ It was previously suggested that classical activated microglia (M1) might be less able to properly uptake A β while alternatively activated microglia (M2) are more efficient phagocytes.⁴⁸ Several in vitro and in vivo studies have provided evidence for the degradation of A β aggregates by microglia.^{49–51} The ability of microglia to digest A β deposits is impaired during progression of the AD.^{45,50} Therefore, it is plausible that improved A β uptake by microglia would ameliorate the progression of the disease. Our results suggest that candesartan, in addition to its anti-inflammatory properties, may

FIGURE 6 Candesartan induced A β_{1-42} phagocytosis by BV2 and primary microglial cells. Cells were incubated with SFM for 20 h followed by 2-h incubation with elevated concentrations of Hilyte Fluor 488-labeled A β_{1-42} (A β). BV2 cells were harvested, and the percentage of A β_{1-42} -labeled positive cells was measured using flow cytometry (A). BV2 (B–C) or primary microglial (D–F) cells were pre-incubated in the presence or absence of 1 or 5 μ mol/L candesartan (Can) with or without 10 μ mol/L cytochalasin D (Cyto D) for 20 h, followed by a 2-h incubation with 0.5 μ mol/L Hilyte Fluor 488-labeled A β_{1-42} (A β) in the presence or absence of 10 μ mol/L cytochalasin (Cyto D) (for BV2) or 0.75 μ mol/L Hilyte Fluor 488-labeled A β_{1-42} (A β) (for primary microglia). Primary microglia gating (D) was obtained using cells staining with rat anti-CD11b/c-PE-Vio-770 and anti-CD45-APC antibodies. Representative images of flow cytometric analysis for phagocytosis by BV2 (B) or primary microglia (E) and the corresponding statistic results (C and F, respectively) are shown. Means \pm SEM of representatives of 3 independent experiments are presented ($n = 3$, each experiment included 3–4 samples of each treatment). One-way ANOVA and a Tukey-Kramer multiple comparison test were used to test for statistical significance. *** $P < 0.001$ vs control (nontreated cells); ^^^ $P < 0.001$ vs A β ; ^ $P < 0.05$ vs A β ; ### $P < 0.001$ vs A β +Can 1 μ mol/L; **** $P < 0.001$ vs A β +Can 5 μ mol/L



shift the microglial activation phenotype toward neuroprotection. Indeed, candesartan treatment not only reduced expression levels of the iNOS and COX-2 in LPS-induced BV2 cells (Figure 3A,B), but also increased expression levels of ARG-1 protein (Figure 3C) and phagocytosis of A β ₁₋₄₂ peptides also in primary microglial cells (Figure 6). It is well established that neuroprotective effects mediated by ARBs, including candesartan, also depend on their agonism for the neuroprotective nuclear receptor peroxisome proliferator-activated receptor (PPAR- γ).^{13,16} Not surprisingly, enhanced phagocytosis of A β peptides by microglia was reported following activation of this receptor.⁵²

A β peptides can be degraded by glial proteases.⁵³ IDE and NEP were reported to be metalloendopeptidases involved in A β peptide cleavage.^{53,54} As candesartan reduced A β in 5XFAD mice, we hypothesized that an increase in NEP and IDE expression would be observed following candesartan treatment. However, no changes in IDE or NEP expression levels in 5XFAD mice brains following candesartan treatment were observed.

Candesartan treatment was previously reported to modulate oligomerization of A β peptides *in vitro*.⁵⁵ However, its effect on A β load was hardly investigated previously, let alone in AD mice model. Administration of candesartan to LPS-injected spontaneously hypertensive rats was shown to reverse amyloidogenesis in the cortical and hippocampal layers.⁵⁶ The present study, conducted on 5XFAD mice, showed that 2-month intranasal treatment with candesartan resulted in reduced A β deposits and microglial accumulation in the hippocampus but not in the cortex (Figure 4). This may result from different age-related and area-dependent expression levels of amyloid burden and gliosis in 5XFAD mouse brains. Initially, young 5XFAD mice exhibit A β pathology and microglial accumulation in the cortex, and as the mice age, amyloid deposits are also observed in the hippocampus.⁹ It seems that robust expression of A β and gliosis is harder to modulate by intranasal candesartan (as indicated in the cortex layer of 5XFAD mice in Figure 4). However, as intranasal candesartan reduced A β deposition in the hippocampus of young (4-month-old) 5XFAD mice (Figure 4), and considering that candesartan was shown to ameliorate AD-related risk factors,^{14,51,52,57} candesartan might be considered as a drug for the early stages of AD. Nevertheless, shorter (3 weeks) intranasal treatment with candesartan resulted in reduced CD11b but not A β expression in the cortex of 5XFAD mice (data not shown). Hence, we assume that the modulatory effect of candesartan on cortical microglial activation precedes later changes of amyloid burden and gliosis observed in different brain areas. In this context, we previously also demonstrated a significant effect of telmisartan, a potent ARB, on gliosis and amyloid burden in age-matched 5XFAD mice in the early stages of the disease.¹⁹ It should be noted that despite promising advantages, chronic intranasal delivery may have some limitations, including poor drugs permeability across nasal epithelium, mucociliary clearance, and irritation or damage to the nasal mucosa.⁵⁸ The first 2 mentioned limitations can be minimized by mucoadhesive formulations or usage of chemical penetration enhancers, improving the bioavailability of drugs that are

incorporated.⁵⁹ Mucosal epithelial damage prevention seems to be one of the main challenges of intranasal administration, and to date, this problem awaits solution. Nevertheless, it should be noted that oral administration also has its own limitations including incomplete drug delivery, increased drug-drug interactions, and exposure to first pass effect.

5 | CONCLUSIONS

This study demonstrated that blockage of AT1R using candesartan, a potent ARB compound, results in an anti-inflammatory effect on microglia and AD mice brains. This effect was accompanied by a shifting of microglia toward a more neuroprotective phenotype and induced phagocytosis of the A β ₁₋₄₂. Taken together with the ability of candesartan to prevent AD risk factors, one could envision potential intervention in glial activation and AD by this compound.

CONFLICT OF INTEREST

The authors declare that the research was conducted in the absence of any commercial or financial relationships that could be construed as a potential conflict of interest.

ORCID

Sigal Fleisher-Berkovich  <http://orcid.org/0000-0002-0797-8816>

REFERENCES

- Block ML, Hong JS. Microglia and inflammation-mediated neurodegeneration: multiple triggers with a common mechanism. *Prog Neurobiol*. 2005;76:77-98.
- ElAli A, Rivest S. Microglia in Alzheimer's disease: a multifaceted relationship. *Brain Behav Immun*. 2016;55:138-150.
- Spangenberg EE, Green KN. Inflammation in Alzheimer's disease: lessons learned from microglia-depletion models. *Brain Behav Immun*. 2017;61:1-11.
- Condello C, Yuan P. Microglia constitute a barrier that prevents neurotoxic protofibrillar Abeta42 hotspots around plaques. *Nat Commun*. 2015;6:6176.
- Mandrekar S, Jiang Q. Microglia mediate the clearance of soluble Abeta through fluid phase macropinocytosis. *J Neurosci*. 2009;29:4252-4262.
- Hamelin L, Lagarde J, Dorothee G, et al. Early and protective microglial activation in Alzheimer's disease: a prospective study using 18F-DPA-714 PET imaging. *Brain*. 2016;139:1252-1264.
- Ano Y, Dhata A, Taniguchi Y, et al. Iso-alpha-acids, bitter components of beer, prevent inflammation and cognitive decline induced in a mouse model of Alzheimer's disease. *J Biol Chem*. 2017;13:763813.
- Malm T, Mariani M. Activation of the nuclear receptor PPARdelta is neuroprotective in a transgenic mouse model of Alzheimer's disease through inhibition of inflammation. *J Neuroinflammation*. 2015;12:014-0229.
- Oakley H, Cole SL, Logan S, et al. Intraneuronal beta-amyloid aggregates, neurodegeneration, and neuron loss in transgenic mice with five familial Alzheimer's disease mutations: potential factors in amyloid plaque formation. *J Neurosci*. 2006;26:10129-10140.

10. Sparks MA, Crowley SD. Classical renin-angiotensin system in kidney physiology. *Compr Physiol*. 2014;4:1201-1228.
11. McKinley MJ, Albiston AL, Allen AM, et al. The brain renin-angiotensin system: location and physiological roles. *Int J Biochem Cell Biol*. 2003;35:901-918.
12. Johnston CI. Biochemistry and pharmacology of the renin-angiotensin system. *Drugs*. 1990;39(Suppl 1):21-31.
13. Saavedra JM. Angiotensin II AT(1) receptor blockers ameliorate inflammatory stress: a beneficial effect for the treatment of brain disorders. *Cell Mol Neurobiol*. 2012;32:667-681.
14. Wright JW, Harding JW. Brain renin-angiotensin—a new look at an old system. *Prog Neurobiol*. 2011;95:49-67.
15. Wright JW, Harding JW. The brain renin-angiotensin system: a diversity of functions and implications for CNS diseases. *Pflugers Arch*. 2013;465:133-151.
16. Saavedra JM. Evidence to consider angiotensin II receptor blockers for the treatment of early Alzheimer's disease. *Cell Mol Neurobiol*. 2016;36:259-279.
17. Saavedra JM, Sanchez-Lemus E, Benicky J. Blockade of brain angiotensin II AT1 receptors ameliorates stress, anxiety, brain inflammation and ischemia: therapeutic implications. *Psychoneuroendocrinology*. 2011;36:1-18.
18. Torika N, Asraf K. Intranasal telmisartan ameliorates brain pathology in five familial Alzheimer's disease mice. *Brain Behav Immun*. 2017;64:80-90.
19. Torika N, Asraf K. Telmisartan modulates glial activation. In vitro and in vivo studies. *PLoS ONE*. 2016;11:e0155823.
20. Saavedra JM. Beneficial effects of angiotensin II receptor blockers in brain disorders. *Pharmacol Res*. 2017;125 (Part A):91-103.
21. Danielyan L, Klein R, Hanson LR, et al. Protective effects of intranasal losartan in the APP/PS1 transgenic mouse model of Alzheimer disease. *Rejuvenation Res*. 2010;13:195-201.
22. Ongali B, Nicolakakis N, Tong XK, et al. Angiotensin II type 1 receptor blocker losartan prevents and rescues cerebrovascular, neuropathological and cognitive deficits in an Alzheimer's disease model. *Neurobiol Dis*. 2014;68:126-136.
23. Wang J, Ho L, Chen L, et al. Valsartan lowers brain beta-amyloid protein levels and improves spatial learning in a mouse model of Alzheimer disease. *J Clin Invest*. 2007;117:3393-3402.
24. Fujisaka S, Usui I, Kanatani Y, et al. Telmisartan improves insulin resistance and modulates adipose tissue macrophage polarization in high-fat-fed mice. *Endocrinology*. 2011;152:1789-1799.
25. Ma LJ, Corsa BA, Zhou J, et al. Angiotensin type 1 receptor modulates macrophage polarization and renal injury in obesity. *Am J Physiol Renal Physiol*. 2011;300:F1203-F1213.
26. Liu J, Zhang PS, Yu Q, et al. Losartan inhibits conventional dendritic cell maturation and Th1 and Th17 polarization responses: novel mechanisms of preventive effects on lipopolysaccharide-induced acute lung injury. *Int J Mol Med*. 2012;29:269-276.
27. Labandeira-Garcia JL, Rodriguez-Perez AI. Brain renin-angiotensin system and microglial polarization: implications for aging and neurodegeneration. *Front Aging Neurosci*. 2017;9:129.
28. Xu Y, Xu Y, Wang Y, et al. Telmisartan prevention of LPS-induced microglia activation involves M2 microglia polarization via CaMKKbeta-dependent AMPK activation. *Brain Behav Immun*. 2015;50:298-313.
29. Garrido-Gil P, Joglar B. Involvement of PPAR-gamma in the neuroprotective and anti-inflammatory effects of angiotensin type 1 receptor inhibition: effects of the receptor antagonist telmisartan and receptor deletion in a mouse MPTP model of Parkinson's disease. *J Neuroinflammation*. 2012;9:38.
30. Sathya S, Ranju V, Kalaivani P, et al. Telmisartan attenuates MPTP induced dopaminergic degeneration and motor dysfunction through regulation of alpha-synuclein and neurotrophic factors (BDNF and GDNF) expression in C57BL/6J mice. *Neuropharmacology*. 2013;73:98-110.
31. Elkahlon AG, Hafko R. An integrative genome-wide transcriptome reveals that candesartan is neuroprotective and a candidate therapeutic for Alzheimer's disease. *Alzheimers Res Ther*. 2016;8:5.
32. Nishimura Y, Ito T. Chronic peripheral administration of the angiotensin II AT(1) receptor antagonist candesartan blocks brain AT(1) receptors. *Brain Res*. 2000;871:29-38.
33. Benicky J, Sanchez-Lemus E, Honda M, et al. Angiotensin II AT1 receptor blockade ameliorates brain inflammation. *Neuropsychopharmacology*. 2011;36:857-870.
34. Benicky J, Sanchez-Lemus E. Anti-inflammatory effects of angiotensin receptor blockers in the brain and the periphery. *Cell Mol Neurobiol*. 2009;29:781-792.
35. Noda A, Fushiki H, Murakami Y, et al. Brain penetration of telmisartan, a unique centrally acting angiotensin II type 1 receptor blocker, studied by PET in conscious rhesus macaques. *Nucl Med Biol*. 2012;39:1232-1235.
36. Tejera D, Heneka MT. Microglia in Alzheimer's disease: the good, the bad and the ugly. *Curr Alzheimer Res*. 2016;13:370-380.
37. Nebel C, Aslanidis A. Activated microglia trigger inflammasome activation and lysosomal destabilization in human RPE cells. *Biochem Biophys Res Commun*. 2017;1:30244-30249.
38. Tahara K, Kim HD. Role of toll-like receptor signalling in Abeta uptake and clearance. *Brain*. 2006;129(Pt 11):3006-3019.
39. Liu Y, Walter S, Stagi M, et al. LPS receptor (CD14): a receptor for phagocytosis of Alzheimer's amyloid peptide. *Brain*. 2005;128(Pt 8):1778-1789.
40. Tonelli LH, Postolache TT. Tumor necrosis factor alpha, interleukin-1 beta, interleukin-6 and major histocompatibility complex molecules in the normal brain and after peripheral immune challenge. *Neurol Res*. 2005;27:679-684.
41. Griffin WS. Inflammation and neurodegenerative diseases. *Am J Clin Nutr*. 2006;83:470s-474s.
42. Bhat SA, Goel R. Angiotensin receptor blockade modulates NFkappaB and STAT3 signaling and inhibits glial activation and neuroinflammation better than angiotensin-converting enzyme inhibition. *Mol Neurobiol*. 2016;53:6950-6967.
43. Bettelli E, Oukka M. T(H)-17 cells in the circle of immunity and autoimmunity. *Nat Immunol*. 2007;8:345-350.
44. Lanz TV, Ding Z, Ho PP, et al. Angiotensin II sustains brain inflammation in mice via TGF-beta. *J Clin Invest*. 2010;120:2782-2794.
45. Mandrekar-Colucci S, Landreth GE. Microglia and inflammation in Alzheimer's disease. *CNS Neurol Disord Drug Targets*. 2010;9:156-167.
46. Colton CA, Mott RT. Expression profiles for macrophage alternative activation genes in AD and in mouse models of AD. *J Neuroinflammation*. 2006;3:27.
47. Sonoki T, Nagasaki A, Gotoh T, et al. Coinduction of nitric-oxide synthase and arginase I in cultured rat peritoneal macrophages and rat tissues in vivo by lipopolysaccharide. *J Biol Chem*. 1997;272:3689-3693.
48. Koenigsnecht-Talboo J, Landreth GE. Microglial phagocytosis induced by fibrillar beta-amyloid and IgGs are differentially regulated by proinflammatory cytokines. *J Neurosci*. 2005;25:8240-8249.
49. Paresce DM, Chung H. Slow degradation of aggregates of the Alzheimer's disease amyloid beta-protein by microglial cells. *J Biol Chem*. 1997;272:29390-29397.
50. Akiyama H, Barger S, Barnum S, et al. Inflammation and Alzheimer's disease. *Neurobiol Aging*. 2000;21:383-421.
51. Hellwig S, Brioschi S, Dieni S, et al. Altered microglia morphology and higher resilience to stress-induced depression-like behavior in CX3CR1-deficient mice. *Brain Behav Immun*. 2016;55:126-137.
52. Yamanaka M, Ishikawa T. PPARgamma/RXRalpha-induced and CD36-mediated microglial amyloid-beta phagocytosis results in cognitive improvement in amyloid precursor protein/presenilin 1 mice. *J Neurosci*. 2012;32:17321-17331.

53. Selkoe DJ. Clearing the brain's amyloid cobwebs. *Neuron*. 2001;32:177-180.
54. Leissring MA, Farris W, Chang AY, et al. Enhanced proteolysis of beta-amyloid in APP transgenic mice prevents plaque formation, secondary pathology, and premature death. *Neuron*. 2003;40:1087-1093.
55. Zhao W, Wang J, Pasinetti, Identification of antihypertensive drugs which inhibit amyloid-beta protein oligomerization. *J Alzheimers Dis*. 2009;16:49-57.
56. Goel R, Bhat SA. Angiotensin II receptor blockers attenuate lipopolysaccharide-induced memory impairment by modulation of NF-kappaB-mediated BDNF/CREB expression and apoptosis in spontaneously hypertensive rats. *Mol Neurobiol*. 2017;18:017-0450.
57. Ries M, Sastre M. Mechanisms of Abeta clearance and degradation by glial cells. *Front Aging Neurosci*. 2016;8:160.
58. Illum L. Nasal drug delivery—possibilities, problems and solutions. *J Control Release*. 2003;87:187-198.
59. Pires A, Fortuna A. Intranasal drug delivery: how, why and what for? *J Pharm Pharm Sci*. 2009;12:288-311.

How to cite this article: Torika N, Asraf K, Apte RN, Fleisher-Berkovich S. Candesartan ameliorates brain inflammation associated with Alzheimer's disease. *CNS Neurosci Ther*. 2018;24:231–242.
<https://doi.org/10.1111/cns.12802>